

# A BIO-INSPIRED CONTRAST ADAPTATION MODEL AND ITS APPLICATION FOR AUTOMATIC LANE MARKS DETECTION

Valiantsin Hardzeyeu and Frank Klefenz

*Fraunhofer Institute for Digital Media Technology, Langewiesener str. 22, 98693, Ilmenau, Germany*

**Keywords:** Retina, contrast adaptation, visual perception, fuzzy-like sets, lane marks detection.

**Abstract:** Even in significant light intensity fluctuations human beings still can sharply perceive the surrounding world under various light conditions: from starlight to sunlight. This process starts in the retina, a tiny tissue of a quarter of a millimeter thick. Based on retinal processing principles, a bio-inspired computational model for online contrast adaptation is presented. The proposed method is developed with the help of the fuzzy theory and corresponds to the models of the retinal layers, their interconnections and intercommunications, which have been described by neurobiologists. The retinal model has been coupled in the successive stage with the Hough transformation in order to create a robust lane marks detection system. The performance of the system has been evaluated with the number of test sets and showed good results.

## 1 INTRODUCTION

Human beings get a significant part of information through the visual perception system which consists of the retina, the visual nerve and the visual cortex in the midbrain. The retina in this sequence plays the role of a pre-processor and reduces the information delivered to the visual cortex. In this paper we like to point out how the retina adapts the intensity fluctuations that appear in the real-life situations and describe a method for the contrast adaptation with the help of the fuzzy-like sets.

According to the work that is presented in (Hubel, 1995) and (Masland, 2001), the retina is a part of the brain, which has been separated from it during the early stages of development, but having kept the connections to the brain through the optic nerve. Five different types of cells form the retina: photoreceptors, horizontal cells, bipolar cells, amacrine cells and ganglion cells. They all are organized in a layered structure and the visual data flows from the upper layer (photoreceptors) to the lower layer (ganglion cells) in a parallel manner. Their interconnections are well described in (Hubel, 1995). Among the other important functions of the retina, like edge extraction and motion detection (Olveczky et al., 2003), the real-time implementation of the contrast adaptation seems to be important for almost all image processing and robotic projects.

As described in (Smirnakis et al., 1997), the contrast adaptation process begins in the lower layers of the retina (amacrine and ganglion cells) and allows the retinal neurons to use their dynamic range more efficiently. The recovery time of the visual system after changing the ambient intensity is several seconds (Baccus and Meister, 2002) and in the (Solomon et al., 2004) were reported that when the mean intensity increase, the retina becomes less sensitive. These biological principles for the contrast adaptation were taken as a basis for the development.

As it pointed out in (Wilson, 1993), the contrast adaptation process which takes place in the retina can be described with help of differential equations. As an alternative, we found a method to describe this non-linear process with fuzzy-like sets and coupled the system with the Hough transform for lane marks detection.

## 2 RETINA MODEL FOR CONTRAST ADAPTATION

Five different layers (three vertical and two horizontal) build up the retina. Vertical layers are presented by photoreceptors (rods and cones), bipolar and ganglion cells and form the *direct pathway* of the visual data flow. Horizontal layers of the retina are presented by the horizontal and

amacrine cells and, together with the vertical layers form the *indirect pathway*. Both paths are needed for the sufficient visual information pre-processing and for forming the signals to the inner brain.

### 2.1 Two Layers, Three Processing Tasks

The cells in the inner retina are organized in a parallel manner and build together a highly distributed structure. In fig. 1 the digital representation of all five retinal cells and their interconnections is shown.

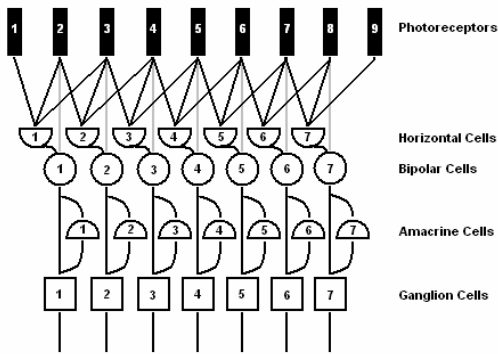


Figure 1: Digital representation of the retinal layers.

All retinal cells can be divided into two processing layers by their functionality. The first layer is presented by the photoreceptors, horizontal and bipolar cells, and performs the edge extraction (Hubel, 1995), (Olveczky et al., 2003), while the second layer, which is formed by the amacrine and ganglion cells, performs among other tasks the local motion detection and the direction of movement estimation (Masland, 2001), (Berry II et al., 1999). Since the contrast adaptation also begins in the lower retinal layers (amacrine and ganglion cells), it is important to understand the responses from the higher processing layers (photoreceptors – bipolars).

### 2.2 Modelling of the Bipolar Cells Response

The processing on the first layers starts from photoreceptors that sense the incoming light. Some of the photoreceptors are activated by the presence of light while others are activated when they do not detect light. All of them are arranged in a circular way so that one type is surrounded by other types (center-surround organization). In this paper we use the ‘on-center’ surrounding organization scheme (Hubel, 1995).

On the next level, the horizontal cells get their input from the photoreceptors. They play a very important role in reducing the amount of information that is given to the inner brain and represent an additional mechanism which helps to adjust the retina response to the overall level of illumination. Their task is to measure the illumination across a broad region of photoreceptors and pass the average value further to the next level. Such calculation can be represented by Equation 1, where  $P_k$  is the output of each photoreceptor that is connected to a horizontal cell  $H_i$ ;  $n$  is the number of inputs of a certain horizontal cell.

$$H_i = \frac{\sum_{k=1}^n P_k}{n} \tag{1}$$

On the third level, the bipolar cells get their inputs from the center photoreceptors directly and from the surrounding photoreceptors indirectly through the horizontal cells. These two inputs build the *receptive field* of each bipolar cell.

The function of the bipolar cell involves a subtraction mechanism: it subtracts the value of the horizontal cell  $H$  from the value which is received from the center photoreceptors. Thus, the output of each bipolar cell  $B_i$  can be represented by the Equation 2, where  $B_{i1}$  is the input from the photoreceptors and the  $B_{i2}$  – is the input from the horizontal cell  $H_i$ .

$$B_i = B_{i1} - B_{i2} \tag{2}$$

The output of each bipolar cell forms the response from the whole receptive field and in this stage retina performs the edge extraction function (Olveczky et al., 2003). As it is known from the classical theory for image processing (Shapiro, 2001), the edge detection operators highlight the boundaries between regions of different intensities. This is, naturally, how human beings perceive the perimeter of an object, when it differs by its intensity from the background. In fig. 2 the stimuli with a step-change border and a simplified model of the first stages of the retina are presented. Here we assume that each photoreceptor corresponds to a single pixel in the image and each bipolar cell  $B$  is driven by the receptive field which is constructed by three photoreceptors – one for the center response and two for the surrounding. The receptive fields of the different bipolar cells overlap each other (Hubel, 1995) and, thus, each photoreceptor is fed not only to the single bipolar cell, but to a number of bipolar cells.

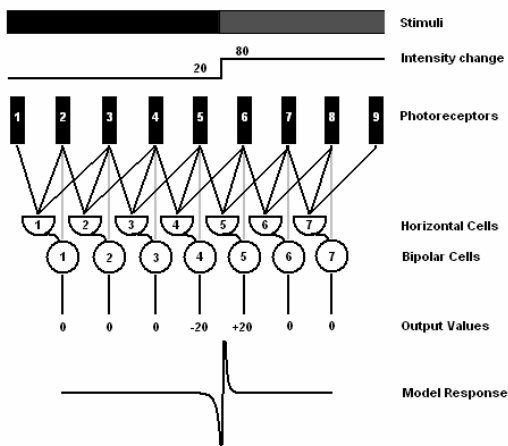


Figure 2: The model and its edge response.

In this example the stimuli change their intensities between the receptors 5 and 6 from 20 to 80. The model's response on the step-change border can be presented by the activities of the two peaks (negative and positive) exactly at the border between the two regions. The absolute values of the peaks are equal, but differ by the sign. Such bio-inspired edge extraction technique called *zero-crossing* has been confirmed by Marr (Marr, 1982) while investigating the neurobiological background of vision. Fig. 3 shows the response of the bipolar cells at vertical edges.

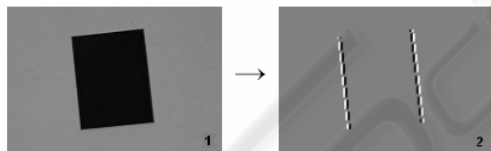


Figure 3: The stimuli and the bipolar cell's response at vertical edges.

The bipolar cells are fed to the amacrine and ganglion cells, but first the signal from the bipolar cell reaches the Contrast Adaptive Neuron.

### 2.3 Contrast Adaptive Neuron and its Function

According to (Smirnakis et al., 1997), when the mean intensity of ambient light increases, the retina becomes less sensitive. This process is organized with the help of the contrast adaptive neuron (CAN), which is located just after the bipolar cells and serves to adjust the input activity of the ganglion cells in order to use their dynamic range more efficiently. In fig. 4 the simplified model of the

receptive field for a single 'on-center' ganglion cell with a CAN is presented.

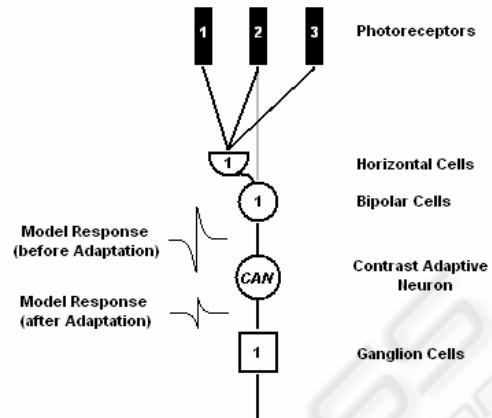


Figure 4: The model of the ganglion cell's receptive field with CAN.

For fig. 4 we assume that the response generated by the bipolar cell lies above the ganglion cell's dynamic range and the CAN brings the bipolar cell response back to the dynamic range of the ganglion cell by changing its amplitude value. However, the retina adapts the high and low intensities differently.

When the contrast changes from low to high (positive contrast change, e.g., going from normal light room conditions to the strong sun light at midday), in the first tens of a second the retina decreases the sensitivity of CAN dramatically, that results in a quick decrease of the ganglion cell's activity. Such first step of the adaptation process is called "*Fast adaptation*" and helps to bring the ganglion cell input nearly to its normal input range. After that the second "*Slow adaptation*" phase occurs and lasts for about ten-fifteen seconds. Its main task is to fine tune the input of the ganglion cell and bring it completely to the middle point of the ganglion cell's dynamic range.

In case, when the contrast changes from high to low (negative contrast change, e.g., going from sun light to the room with normal light conditions), the retina reacts differently. There is no fast adaptation process, but the retina increases step-by-step the sensitivity of the ganglion cells by scaling up their inputs (with help of CAN). It takes up to twenty-twenty five seconds till the inputs of the ganglion cells are in their dynamic range.

These two statements were confirmed by Solomon et al (Solomon et al., 2004) while observing the reaction of the isolated retina of a tiger salamander during contrast changes. Fig. 5 shows the adaptation process for negative and positive contrast changes.

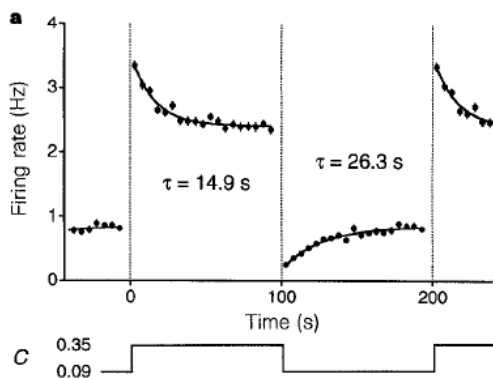


Figure 5: Contrast adaptation in salamander's retina from (Solomon et al., 2004).

In fig. 5 C depicts the contrast change values while the graphical representation shows the adaptation in the Salamanders retina on different contrast changes.

We investigated which functions might approximate the curves for "negative" and "positive" adaptation and found out that for the approximation of the "positive" contrast adaptation process (fig. 6a, upper image) a simple *rational function* (fig. 6b, upper image) can be used. "Negative" contrast adaptation curve (fig. 6a, lower image) can be approximated by the *square root function*, which is shown in fig. 6b (lower image).

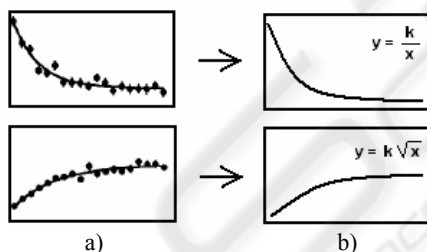


Figure 6: a) Natural adaptation curves (from (Solomon et al., 2004)) and b) their approximation functions.

Here, in both functions the coefficient  $k$  is a scaling factor, which is responsible for the *CAN's* selectivity. It controls how strong the adaptation should be in order to make the ganglion cells more or less sensitive, depending on the current light intensity situation. For instance, when the light intensity is high (e.g., in sunny midday) than the *CAN* should scale the intensity down by setting a rather large  $k$ ; however, when the light intensity is just a bit above the dynamic range, the *CAN* should fine tune the contrast by setting a quite small value for the scaling coefficient. In this work we use the fuzzy-like sets for the definition of *CAN's* selectivity coefficient  $k$ .

### 3 USING FUZZY-LIKE SETS FOR CONTRAST ADAPTATION

In recent decades a number of applications were found for fuzzy logic in economics, mathematics and engineering. Firstly introduced in (Zadeh, 1965), it is very helpful for modelling highly nonlinear processes like natural contrast adaptation

#### 3.1 Definition of a Fuzzy – like Set for Normal Contrast

For the graphical representation of the model's response we should declare, what the Normal contrast means and create a corresponding fuzzy – like set for its definition.

Since we are working with bio-inspired edge extraction based on zero-crossings, we assume here that the absolute zero, as it shown on the characteristic curve in fig. 2 will be equal to the intensity 128, which represents the middle point of the intensity spectrum. When model analyzes the border between object and background, on the graphical representation the response will drop down and then raise up by a certain value (e.g., dark and light vertical lines in fig. 3, image 2).

Then we analyzed which intensity differences can represent the Normal Contrast value (see fig.7).

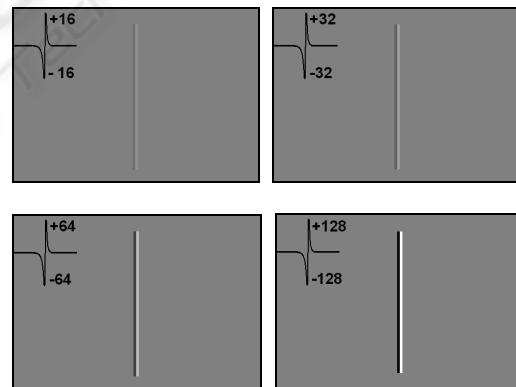


Figure 7: Biological edges with 16, 32, 64 and 128 intensity difference levels.

Fig. 7 shows four biological edges with intensities 16, 32, 64 and 128. The edges with the intensity differences of 16 and 32 do not have enough contrast and should be adapted. The edges with intensity difference of 64 and 128 do have enough contrast and thus there is no need for adaptation. However, in the real world situation the biological intensity difference of 128 is hardly possible, because it causes an intensity change of 255 levels at the object-background border (e.g.,

changing from black to white). Normally the contrast numbers, which can be detected in real images, lie in the range from 120 to 200, which caused the biological edge of  $[\pm 60 - \pm 100]$  to appear. That is why we do not have to adapt the high intensity values (e.g., from 180 to 255), we should only define such a process, which will adapt the edge values from the lower part of the intensity difference spectrum and bring them in to the middle region. Thus, only the “negative” contrast adaptation process should be used (fig. 6, lower images).

Following this, we introduce a Normal Contrast fuzzy variable which should adapt all the values that lie under the intensity 60. It is presented in fig. 8.

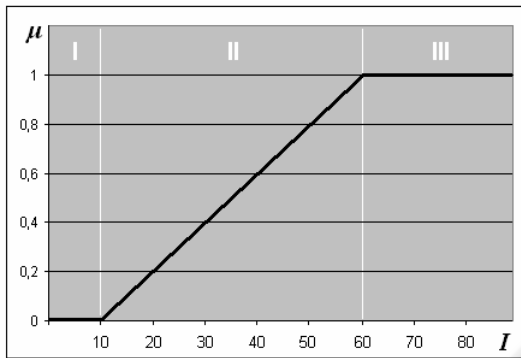


Figure 8: Fuzzy variable for Normal Contrast.

On this image, the X-axis represents the intensity change  $I$  on the biological edge and Y-axis shows the membership  $\mu$  of a certain intensity value in the Normal Contrast variable.

There are three characteristic adaptation regions presented on this graphic. Since the fuzzy logic operates with linguistic variables, table 1 shows such a linguistic description and action which is needed for a certain region.

Table 1: Linguistic definition of the model.

Region	Intensity	Action needed
I	Low Intensity	Strong adaptation
II	Low-to-Normal Intensity	Adaptation based on the $\mu$ membership coefficient in order to control adaptation strength
III	Normal Intensity	No adaptation needed

When the bipolar cells deliver low intensities (values from 1 to 10), strong adaptation is needed; in the mid-range (values from 11 and 60), adaptation is also needed, but the system should control the strength of the adaptation by using the membership

coefficient  $\mu$ ; and when the intensity is normal (values above 61), then no adaptation is needed.

In order to create the system we should define the set of rules for each of the regions mathematically. Since we are using the “negative” adaptation process, a curve that will represent this process should have the shape of the *square root* function. Table 2 shows the mathematical representation for each action regions.

Table 2: Mathematical representation of the model.

Region	Intensity values	Representation
I	1 – 10	$K = 2 \cdot \sqrt{x}$ $I_{new} = I_i \cdot K$
II	11 – 60	$\mu = (2 \cdot I_i + 20) / 100$ $K = (2 - \mu) \cdot \sqrt{x}$ $I_{new} = I_i \cdot K$
III	61 – 127	$I_{new} = I_i$

The adaptation process in nature lasted for several seconds. Here this process is modelled with iteration mechanism and  $x$  represents current iteration;  $K$  is an adaptation coefficient and should be calculated differently for regions I, II and III. It represents the *CAN* selectivity and controls the input gain to the ganglion cells.  $I_i$  represents the input intensity of *CAN* and  $I_{new}$  is a new calculated value of the adapted intensity;  $\mu$  is a membership coefficient, which influences the amplification factor and is calculated according to the equation of the characteristic line in region II (see fig. 8).

### 3.2 Adaptation Algorithm

The algorithm for the contrast adaptation involves all the definition for the variables that have been set early, like  $I_i$ ,  $I_{low}$ ,  $I_{normal}$ ,  $I_{new}$ ,  $\mu$ ,  $K$  and  $x$  which is initially set to 0. Firstly, based on the current intensity  $I_i$ ,  $\mu$  is calculated.

```

if ( $I_i > 1$  &&  $I_i \leq I_{low}$ ) {  $\mu = 0$  }
if ( $I_i > I_{low}$  &&  $I_i \leq I_{normal}$ ) {
     $\mu = (2 \cdot I_i + 20) / 100$  }
if ( $I_i > I_{normal}$ ) {  $\mu = 1$  }
    
```

Then the adaptation coefficient  $K$  and the adapted intensity  $I_{new}$  based on the equations in table 2 is calculated.

```

if ( $\mu < 1$ ) {
    while ( $I_{new} \leq I_{normal}$ ) {
         $K = (2 - \mu) \cdot \sqrt{x}$ 
         $I_{new} = I_i \cdot K$ 
         $x = x + 1$ ;
    }
}
    
```

else { $I_{new}=I_i$ }

The process stops, when the calculated intensity  $I_{new}$  reaches the normal intensity  $I_{normal}$  that has been set to 60 empirically.

### 3.3 Adaptation Results

During the investigation and development the model has been tested on different types of images. Experiments were divided into three categories by the specific adaptation process:

- adaptation of the low contrast;
- adaptation of the low-to-normal contrast;
- adaptation of the real world images;

The first two categories were tested with synthetic images. Synthetic images were chosen because the results of the processing can be predicted in order to make the model's proof of concept under different conditions. To demonstrate it a number of images with different intensity changes were chosen. Fig. 9 represents two of them.

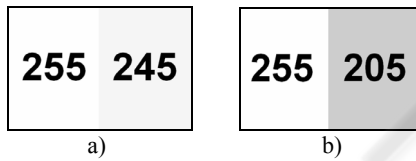


Figure 9: Experimental data.

Fig. 9a shows the intensity change of 10 levels (from 255 to 245) and figure 9b corresponds to a change of 50 levels (from 255 to 205) of the intensity spectrum. The digits on the images represent just the absolute intensities and will not appear in the modelling results.

Fig. 10 shows the calculated bipolar cells activity for fig. 9a and 9b correspondently.



Figure 10: Calculated bipolar cell's responses to the experimental data in fig. 9.

For the first experiment we took fig. 10a. The initial data (fig. 9a) shows minor intensity change at the object-background border, which causes a low contrast and hardly distinguished border response (fig. 10a). The initial intensity change  $I_i$  equals 3 (see equations 1 and 2), which corresponds to the

low intensity region in fig. 8. Initial data:  $I_i = 3; \mu = 0, \Rightarrow K = 2 \cdot \sqrt{x}$ .

For the adaptation of such a low intensity 104 iterations are needed. Table 3 shows some of them.

Table 3: First experiment data.

$x$	$K$	$I_{new}$	Graphical representation
1	2	6	
2	2.82	8	
3	3.46	10	
4	4	12	
...			
101	20.09	60	
102	20.19	60	
103	20.30	60	
104	20.40	61	

The second experiment has been performed with fig. 10b. The initial intensity change here  $I_i$  is 16, which corresponds to the low-to-normal intensity region in fig. 8. Adaptation is still needed, but the strength of the adaptation should be controlled. Initial data:  $I_i = 16; \mu = 0.12, \Rightarrow K = (2 - \mu) \cdot \sqrt{x}$ .

According to the algorithm, the adaptation of such intensity will be done in 5 iteration steps. Table 4 represents this process.

Table 4: Third experiment data.

$x$	$K$	$I_{new}$	Graphical representation
1	1.88	30	
2	2.65	42	
3	3.25	52	
4	3.76	60	
5	4.20	67	

As it can be seen on the results presented above, the contrast adaptation model shows the expected responses on the different stimuli with different adaptation time. The intensity change adaptation correlates with its natural representation (fig. 6, lower image). To confirm this, fig. 11 shows the adaptation curves for each experiment.

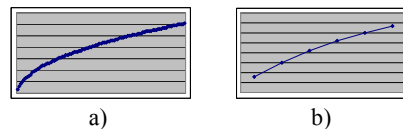


Figure 11: Adaptation curves for all experiments.

### 3.4 Adaptation of the Real World Images

The model has been already tested on the synthetic images; the next step is to see how it will respond on the real world images. For this purpose we choose a number of images with the real road scenes that have been taken on a german highway. Some of these test images are shown in Fig. 12.



Figure 12: Real road scenes.

Then we processed the images first with the classical biological edge operator *without* the contrast adaptation mechanism. On the 2<sup>nd</sup> phase the same images have been processed with the bio-inspired edge operator and *with* the contrast adaptation module. Fig. 13 shows the results.

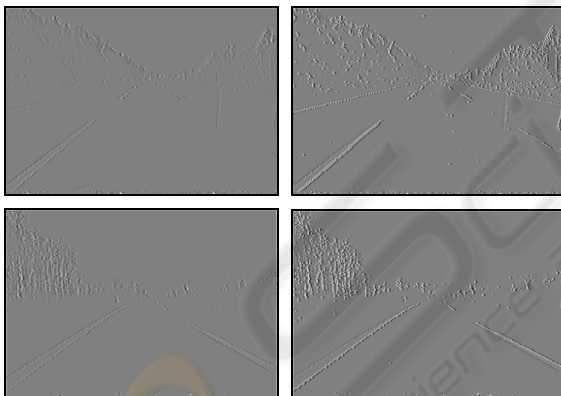


Figure 13: Calculated biological edge without (left) and with (right) contrast adaptation for fig. 12.

The difference between the adapted and the not adapted images can be clearly seen. The edges, that are even not fully visible on the left images, are well seen on the right ones. Besides, the initial images (fig. 12) were taken under slightly different illumination conditions: the first image was taken under bright sun light while the second one at early evening. Nevertheless, the adapted images show good results especially in underlining the lane road marks. This gives the possibility to use this contrast adaptation model for robust lane detection.

## 4 LANE DETECTION APPLICATION

Lane keeping assistant systems have been described in a number of recent publications, e.g. (Risack et al., 2000), (Chang et al., 2003). For such systems detection of the lane marks is a key feature for further processing. The lane marks form lines with certain slopes and thus, for its detection a good shape extraction method is needed.

The Hough transformation (Leavers, 1992) is a pattern recognition technique which is known for its performance in locating given shapes in images. Some researches have reported that the Hough transform correlates with the processes that happen in the striate cortex and in fact, reproduces the natural mechanism of objects contour extraction (Hubel, 1995), (Blasdel, 1992), (Ballard et al., 1983), (Brueckmann et al., 2004).

Very interesting state-of-the-art research work is presented in (Serre, 2007). The authors describe the usage of the midbrain biological mechanisms for the real world scene segmentation and objects recognition. Furthermore, they also use the Hough transformation as a shape localization method.

That is why we propose to use the Hough transform as a lane marks detection method together with the retina model with contrast adaptation as a preprocessing method. This gives the possibility to create a fully bio-inspired system for the lane mark detection. The architecture of such a system is shown in fig. 14.

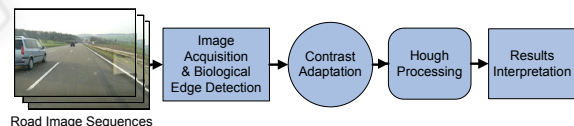


Figure 14: Architecture of the bio-inspired lane detection system.

The biological edge detection and contrast adaptation stages were well described above. In fig. 14, after contrast adaptation the Hough transformation takes place. Hough transformation involves a voting scheme for the shape detection. In particular, here we extract the lines of the different slopes. Fig. 15 represents the Hough spaces built from road edge picture (fig. 13, two right images) and then the maximas are marked.

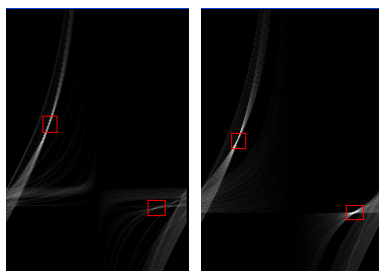


Figure 15: Hough spaces with local maximas.

After the maxima were detected, the interpretation of the results should be performed. Each maximum on the Hough space corresponds to the line with a certain slope in a Cartesian space and after processing the detected lane marks will be highlighted. Fig. 16 shows the final results.

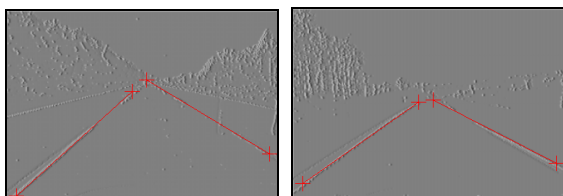


Figure 16: Detected lane marks in the adapted images.

## 5 CONCLUSIONS AND FUTURE WORK

In this paper a bio-inspired model for contrast adaptation has been presented. The model has been tested with different test sets and showed good results. Furthermore, the proposed contrast adaptation algorithm has been coupled with the Hough-based lane marks detector. This coupling showed good performance and full correspondence to the predicted behaviour.

Future work will concentrate on development of the lane keeping assistant system using the bio-inspired techniques further. In particular, for the preprocessing stage the colour perception model will be investigated, implemented and will be used for the road scenes segmentation and traffic signs detection.

Besides, for the post-processing and trajectory prediction stages time-to-lane crossing approach will be taken in to the account. It is likely possible that it might be modelled with the natural timing delay-computational maps. This problem will be also investigated and the results will be reported.

## REFERENCES

- David H. Hubel, *Eye, Brain and Vision*, Freeman, 1995.
- Linda G. Shapiro, George C. Stockman, *Computer Vision*, Prentice-Hall, 2001.
- Bence P. Ölveczky, Stephen A. Baccus & Markus Meister, "Segregation of the object and background motion in the retina," *Nature*, Vol. 423, May 2003, pp. 401 – 408.
- Richard H. Masland, "The fundamental plan of the Retina," *Nature Neuroscience*, Vol.4 No. 9, September 2001, pp. 877 – 886.
- Michael J. Berry II, Iman H. Brivanlou, Thomas A. Jordan & Markus Meister, "Anticipation of moving stimuli by the retina," *Nature*, Vol. 398, March 1999, pp. 334–338.
- Hugh R. Wilson, "Nonlinear processes in the visual discrimination", *Proc. Natl. Acad. Sci. USA*, Vol. 90, 1993, pp. 9785 – 9790.
- Stelios M. Smirnakis, Michael J. Berry, David K. Warland, William Blalek & Markus Meister, "Adaptation of retinal processing to image contrast and spatial scale," *Nature*, Vol. 386, March 1997, pp. 69–73
- Stephan A. Baccus & Markus Meister, "Retina Versus Cortex: Contrast Adaptation in Parallel Visual Pathways", *Neuron*, 2003, pp. 5 – 7.
- Stephan A. Baccus & Markus Meister, "Fast and Slow Contrast Adaptation in Retinal Circuitry," *Neuron*, Vol. 36, 2002, pp. 909 – 919.
- Samuel Solomon, Jonathan Peirce, Neel Dhruv, Peter Lennie, "Profound Contrast Adaptation Early in the Visual Pathway", *Neuron*, vol. 42, 2004, pp. 155–162
- Zadeh L.A., "Fuzzy Sets", *Information and Control*, 1965, vol. 8, pp. 338 - 353.
- Marr D., *Vision*, Freeman, pp. 54 – 78. 1982.
- Risack, R.; Mohler, N.; Enkelmann, W., A video-based lane keeping assistant, *Intelligent Vehicles Symposium*, 2000. Proceedings of the IEEE, pp. 356 – 361, 2000.
- Tang-Hsien Chang; Chun-Hung Lin; Chih-Sheng Hsu; Yao-Jan Wu. A vision-based vehicle behavior monitoring and warning system *Proceedings IEEE*, Volume 1, pp. 448 – 453, 2003.
- Leavers, V.F., *Shape detection in Computer Vision using Hough Transform*. Springer – Verlag, p.201, 1992.
- Gary G. Blasdel, "Orientation Selectivity, Preference, and Continuity in Monkey Striate Cortex", *The Journal of Neuroscience*, Aug. 1992, 12 (8): 3139 – 3161.
- Ballard D., Hinton J., Sejnowski T., Parallel visual computation. *Nature* 306, pp. 21 – 26, 1983.
- T. Serre, L. Wolf, S. Bileschi, M. Riesenhuber, and T. Poggio, "Robust Object Recognition with Cortex-like Mechanisms", *IEEE Trans. on Pattern Analysis and Machine Intelligence*, vol. 29, no. 3, March 2007.
- Brueckmann, A., Klefenz F., Wuensche, A. A neural Net for 2-D Slope and Sinusoidal Shape Detection. *International Scientific Journal of Computing*. Vol. 3 (1), pp. 21 – 26, 2004.